

Robust Earthquake Location using Random Sample Consensus (RANSAC)

Weiqliang Zhu^{*1}, Bo Rong¹, Yaqi Jie², and S. Shawn Wei²

¹Department of Earth and Planetary Science, University of California, Berkeley, Berkeley, CA, USA

²Department of Earth and Environmental Sciences, Michigan State University, MI, USA

Abstract

Accurate earthquake location, which determines the origin time and location of seismic events using phase arrival times or waveforms, is fundamental to earthquake monitoring. While recent deep learning advances have significantly improved earthquake detection and phase picking, particularly for smaller-magnitude events, the increased detection rate introduces new challenges for robust location determination. These smaller events often contain fewer P- and S-phase picks, making location accuracy more vulnerable to false or inaccurate picks. To enhance location robustness against outlier picks, we propose a machine learning method that incorporates the Random Sample Consensus (RANSAC) algorithm. RANSAC employs iterative sampling to achieve robust parameter optimization in the presence of substantial outliers. By integrating RANSAC's iterative sampling into traditional earthquake location workflows, we effectively mitigate biases from false picks and improve the robustness of the location process. We evaluated our approach using both synthetic data and real data from the Ridgecrest earthquake sequence. The results demonstrate comparable accuracy to traditional location algorithms while showing enhanced robustness to outlier picks.

1 Introduction

Earthquake source parameters, including time, location, and mechanism, provide foundational information for understanding earthquake characteristics, fault zone structures, and various subsurface processes associated with volcanoes, glaciers, geothermal energy, oil and gas extraction, and CO₂ sequestration (Kanamori & Brodsky, 2004; Ellsworth, 2013; Faulkner et al., 2010; Shelly et al., 2016). To construct earthquake catalogs and deliver early warning information, seismic networks routinely detect earthquakes and pick phase arrivals to determine origin times and hypocenters (Kanamori, 2005; Allen et al., 2009; Hutton et al., 2010).

The basic mechanism of earthquake location is to find source parameters that best fit observed phase arrival times across a network of stations, based on a velocity model and a travel-time calculation algorithm. The classic approach, i.e., Geiger's method (Geiger, 1912), employs iterative least-squares optimization by linearizing travel-time changes relative to small perturbations in earthquake hypocenters and applies Gauss-Newton nonlinear optimization (Thurber, 1985). Commonly used earthquake location programs such as HYPO71 (Lee & Lahr, 1975) and HYPOINVERSE (Klein, 2002) build upon Geiger's method and operate routinely in earthquake monitoring systems. These programs incorporate various improvements to enhance location quality, including sophisticated weighting schemes for phase arrival qualities, optimized hyperparameters for iteration and damping, and location error estimations.

Advanced algorithms have been developed to accommodate inaccurate velocity models and improve optimization methods with uncertainty quantification. Important techniques include directly inverting earthquake location and velocity model (Lahr, 1979; Thurber, 1983; Kissling et al., 1994; Thurber, 1992), adding

*zhuwq@berkeley.edu

static station corrections (Douglas, 1967; Ellsworth, 1975; Frohlich, 1979; Pujol, 1988; Frohlich, 1979; Lomax, 2005) and source-specific station terms (Richards-Dinger & Shearer, 2000; P. Shearer et al., 2005; Lin & Shearer, 2006; Lin, 2018; Lomax & Savvaidis, 2022), using equal differential travel-times at station pairs (H.-w. Zhou, 1994; Font et al., 2004), using double-difference travel-times for earthquake pairs (Waldhauser & Ellsworth, 2000; Waldhauser, 2001; Trugman & Shearer, 2017), and including location uncertainty estimation using Bayesian optimization (Hirata & Matsu’ura, 1987; Myers et al., 2007; Lomax et al., 2009; Smith et al., 2022). These advancements have significantly improved earthquake location accuracy, enabling detailed seismicity mapping with precise spatiotemporal information for studying complex earthquake sequences, fault zone structures, induced seismicity, volcanic earthquakes, and other geological processes (Waldhauser & Ellsworth, 2002; Waldhauser & Schaff, 2008; Hauksson et al., 2012; Richards-Dinger & Shearer, 2000; Shelly, 2020a; Ross et al., 2020; Park et al., 2022; Wilding et al., 2023; Trugman, 2024).

In addition to these improvements in location accuracy, a critical challenge lies in enhancing location robustness against outliers in arrival-time measurements. This issue has become increasingly significant as detection thresholds continue to lower through advanced detection algorithms such as deep learning-based phase picking models, identifying more earthquake signals from continuous seismic archives (Ross et al., 2018; Mousavi et al., 2020; W. Zhu & Beroza, 2019; Sun et al., 2023). A fundamental trade-off exists between increasing detection numbers and minimizing false positives throughout the earthquake monitoring workflow, from phase detection/picking, phase association, to event location. In the phase detection/picking step, efforts to detect weak signals from small earthquakes that are often near or below noise levels inevitably generate false picks from anthropogenic, instrumental, and natural noise sources. Additionally, arrival time tends to exhibit increased errors in low signal-to-noise ratio (SNR) waveforms, making precise first-arrival picking increasingly challenging. In the phase association step, which clusters picks across seismic networks into individual earthquakes while filtering out false picks, two challenges arise from increasing false picks: First, small earthquakes typically yield limited P- and S-phase arrivals, necessitating lower thresholds for minimum pick numbers per event, which, in turn, increases the chance that false picks may be associated to create false event detections. Second, abundant false picks from background noise increase the likelihood of false picks coincidentally matching true event travel-time moveouts, potentially biasing location results, especially for events with few picks. These errors from phase picking and association steps, including false picks and inaccurate phase arrival times, can accumulate to the earthquake location step, potentially resulting in erroneous or biased location results.

Several approaches have been proposed to improve location robustness, including alternative target functions less sensitive to outliers (e.g., $L1$ -norm loss or Huber loss instead of $L2$ -norm loss) (Anderson, 1982; P. M. Shearer, 1997; Trugman & Shearer, 2017), likelihood functions incorporating uncertainties (Lomax et al., 2000; Smith et al., 2022), and specialized residual weighting and outlier filtering schemes in iterative optimization (Klein, 2002). In this work, we propose combining the Random Sample Consensus (RANSAC) algorithm (Fischler & Bolles, 1981) with earthquake location to enhance robustness against outliers. The RANSAC algorithm is designed for robust parameter estimation in the presence of significant outliers. Instead of minimizing error across all data points, RANSAC aims to maximize the inlier consensus set through randomly sampling multiple subsets that are sufficient to constrain model parameters, thereby effectively isolating and disregarding outliers. RANSAC has been widely applied in computer vision tasks (Hartley & Zisserman, 2003; Szeliski, 2022) and has recently emerged in geophysical applications, including recognizing linear fault planes (Fadakar Alghalandis et al., 2013; Pollitz et al., 2017; X. Liu et al., 2018; Skoumal et al., 2019) and solving phase picking and association tasks (L. Zhu et al., 2016; Woollam et al., 2020; L. Zhu et al., 2017, 2021). These studies directly apply the RANSAC algorithm based on linear curve or hyperbolic curve fitting (L. Zhu et al., 2017). (Trugman et al., 2020) demonstrated improved laboratory earthquake location accuracy by combining grid-searching with RANSAC for outlier pick removal.

Building on RANSAC’s advantages, we present an earthquake location method that integrates RANSAC’s random sampling iteration with traditional optimization processes to achieve robust outlier resistance. We validate our method using both synthetic examples and field data from the 2016 Ridgecrest sequence. The improved robustness to false picks in the location step would enable lower thresholds in earlier steps of phase picking and association for small-magnitude earthquake detection. The enhanced accuracy in earthquake locations ultimately contributes to higher-quality earthquake catalogs, supporting a wide range of geophysical studies.

2 Methods

2.1 Earthquake location

Earthquake localization aims to determine source parameters, origin time and hypocenter, that best fit observed phase arrival times across a network of stations, assuming a velocity model and travel-time calculation function. Travel-times of phase arrivals t are commonly estimated using ray-tracing (Um & Thurber, 1987; Aki & Lee, 1976; D. Zhao et al., 1992; Červený & Pšenčík, 2020) or by solving the eikonal equation (Vidale, 1988; Van Trier & Symes, 1991; Podvin & Lecomte, 1991; Tong, 2021; Smith et al., 2020). In this work, we solve the eikonal equation to calculate travel-time:

$$|\nabla t(x, y, z)| = \frac{1}{v(x, y, z)} \quad (1)$$

$$t(x_0, y_0, z_0) = 0 \quad (2)$$

where $t(x, y, z)$ is the travel-time from hypocenter to station, $v(x, y, z)$ is the velocity model, t_0 is the earthquake origin time, and x_0, y_0, z_0 are the earthquake hypocenter coordinates. We employ the fast-sweeping method to solve the eikonal equation (H. Zhao, 2005), which offers both computational efficiency and straightforward implementation. The phase arrival-time is expressed as the origin time plus travel-time, with an optional station correction term δ_s :

$$\hat{T} = t_0 + t(x, y, z) + \delta_s \quad (3)$$

The objective for earthquake location is to minimize the misfit between observed (T_i) and calculated (\hat{T}_i) phase arrival-times:

$$\mathcal{L} = \sum_{i=1}^N w_i f(\hat{T}_i - T_i) \quad (4)$$

where N is the number of phase measurements, w_i is the weight assigned to each phase pick, and f is the loss function. Common loss functions include $L2$ -norm loss, $L1$ -norm loss, and huber loss (Huber, 1964). We select the Huber loss function in this study, as it is less sensitive to outliers, same as the $L1$ -norm loss and converges quickly for small residuals, akin to the $L2$ -norm loss:

$$f(x) = \begin{cases} \frac{1}{2}x^2 & \text{if } |x| \leq \delta \\ \delta \cdot (|x| - \frac{1}{2}\delta) & \text{if } |x| > \delta \end{cases} \quad (5)$$

The earthquake location process involves minimizing the target function \mathcal{L} to optimize the earthquake origin time t_0 and hypocenter (x_0, y_0, z_0) :

$$\min_{t_0, x_0, y_0, z_0} \mathcal{L} = \sum_{i=1}^N w_i f(t_0 + t(x, y, z) + \delta_s - T_i) \quad (6)$$

Given the non-linearity of the travel-time function, we employ the BFGS quasi-Newton optimizer (Nocedal & Wright, 1999; Byrd et al., 1995) to optimize the target function. The gradient of the target function with respect to hypocenter coordinates can be computed either by interpolating the spatial derivatives of the travel-time field ($\partial t/\partial x$, $\partial t/\partial y$, $\partial t/\partial z$) or through automatic differentiation techniques (Paszke et al., 2017; Baydin et al., 2018; W. Zhu et al., 2021). The gradient with respect to origin time is linear and computed analytically.

2.2 RANSAC-based optimization

The earthquake location process described above assumes reliable picks with residual errors following a Gaussian distribution (for $L2$ -norm loss) or a Laplace distribution (for $L1$ -norm loss). However, phase picks are often contaminated by outliers, especially for small-magnitude earthquakes or in noisy conditions. To improve robustness against outlier picks, we employ the Random Sample Consensus (RANSAC) algorithm (Figure 1). The RANSAC algorithm can be summarized in the following steps:

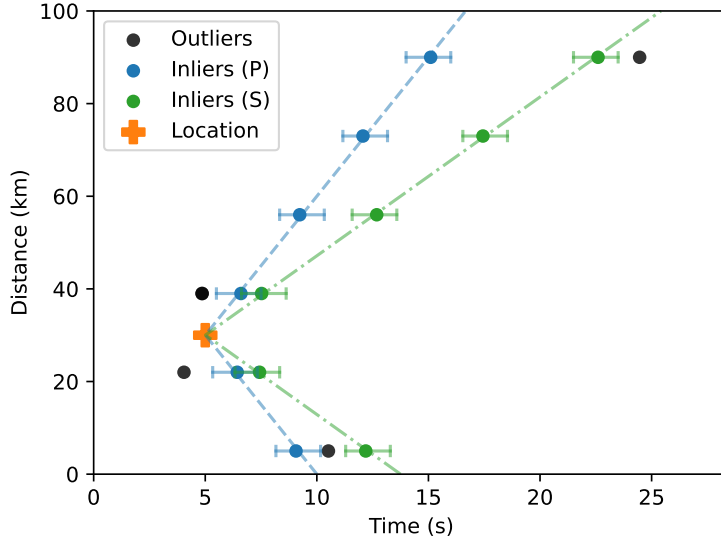


Figure 1: Schematic diagram of the RANSAC-based earthquake location algorithm, which employs iterative sampling to identify and exclude outlier picks while optimizing earthquake location parameters.

1. Randomly sample a subset of phase picks S from the group of picks G ;
2. Evaluate subset quality (e.g., number of P and S picks); if insufficient, resample a new subset;
3. Locate earthquake using the subset S by minimizing target function Equation (6);
4. Apply the model to the group of picks G and compute evaluation metrics (e.g., the number of inliers and residuals);
5. Evaluate model quality; Update the best model if current model is superior;
6. Repeat for K iterations or until meeting predefined stopping criteria (e.g., maximum iterations, maximum number of inliers, or minimum residuals);
7. Use the best inlier subset to determine final earthquake location.

RANSAC’s iterative sampling relies on the assumption that a small subset of picks can adequately constrain model parameters. This assumption is valid for earthquake location because only four free parameters, i.e., origin time and hypocenter coordinates, need to be determined, while the number of picks per event typically exceeds four. Physical constraints in earthquake location inform the selection of RANSAC hyperparameters, such as minimum subset size and maximum allowable residuals. For example, we set the minimum subset size as $\max(S_{min}, \alpha G)$, where S_{min} is the minimum number of picks, and α represents the approximate ratio of true picks within G ; and we set the maximum allowable time residuals to 1 second. These hyperparameters can be optimized based on specific application scenarios.

2.3 Other improvements

Since RANSAC’s iterative sampling process operate independently of the earthquake location optimization, enhancements to earthquake location methods can seamlessly integrate with RANSAC. We demonstrate two improvements: static station corrections and phase amplitude-based outlier detection.

2.3.1 Station correction terms

Static station correction terms are used to account for systematic errors in observed phase arrival-times related to station-specific velocity model inaccuracies. These correction terms can be estimated from residuals between observed and calculated arrival-times for each station:

$$\Delta\delta_s = \sum_{i=1}^N w_i (t_0 + t(x, y, z) + \delta_s - T_i) / \sum_{i=1}^N w_i \quad (7)$$

where N is the number of phase picks, w_i is the pick weight, and $\Delta\delta_s$ is the correction term for station s . We estimate separate station correction terms for P and S phases at each station.

2.3.2 Phase amplitudes for outlier detection

Phase amplitudes, while less precise for constraining locations, can identify outliers in phase picks. Amplitude information enhances phase association (W. Zhu et al., 2022) by distinguishing picks with similar arrival-times but differing amplitudes from earthquakes of varying magnitudes and distances. In conditions with numerous false picks, outliers near travel-time moveouts may bias earthquake locations, but their inconsistent amplitudes can help identify and remove them. During Step 4 of RANSAC, we calculate both travel-time and amplitude residuals:

$$\log A = c_0 + c_1 M + c_2 \log R \tag{8}$$

where A is phase amplitude, M is earthquake magnitude, R is epicentral distance, and c_0 , c_1 , and c_2 are coefficients. Integrating this linear relationship into RANSAC enables outlier detection with minimal computational overhead.

3 Results

To benchmark the performance of the RANSAC-based earthquake location method, we evaluated it using both synthetic examples and the 2016 Ridgecrest earthquake sequence.

3.1 Benchmarking on synthetic datasets

We first evaluated the earthquake location performance using a controlled synthetic experiment developed by Yu et al. (2024). The synthetic datasets of phase picks were generated using the fast-marching method (White et al., 2020) with a 3D velocity model, incorporating realistic picking errors, phase availabilities, and phase outliers to simulate real-world conditions. In their controlled experiment, Yu et al. (2024) compared the performance of commonly used earthquake location algorithms, including Hypoinverse, VELEST, NonLinLoc, NonLinLoc_SSST, and HypoSVI. This synthetic dataset provides an ideal benchmark for evaluating the RANSAC-based earthquake location method, which uses the fast-sweeping method (H. Zhao, 2005) for travel-times calculations and the BFGS optimization method for earthquake location inversion. Figures 2 to 4 show the ground-truth earthquake locations alongside the inverted locations; the estimated static station terms (SST), and filtered outliers using RANSAC, respectively. Table 1 presents a quantitative evaluation of the effects of adding static station terms and RANSAC iterations, compared with other commonly used location methods.

The synthetic dataset results validate the effectiveness of both static station terms and RANSAC iterations. First, the vanilla ADLoc results demonstrate that our implementation using the fast-sweeping eikonal solver for phase travel-time calculations and the BFGS quasi-Newton optimizer for earthquake location optimization works correctly, though as expected, achieves lower accuracy than well-optimized algorithms like Hypoinverse, VELEST, and NonLinLoc. Second, the ADLoc+SST results show that static station terms effectively reduce location bias from inaccurate velocity models, improving accuracy to levels comparable to or better than other location algorithms. The estimated SST for P-phase and S-phase are shown in Figure 3. Third, the ADLoc+SST+RANSAC results achieve the best performance through additional outlier pick removal. Step 4 of the RANSAC iterations effectively detects and removes outlier picks based on customizable thresholds. Without phase amplitude information in the benchmark dataset, we relied only on travel-time residuals for outlier detection. The threshold for maximum travel-time residual, a hyperparameter, can be adjusted based on pick quality. Experiments with thresholds of 1.0s and 0.2s both improved location results, with the tighter 0.2s threshold achieving better performance on this relatively clean benchmark dataset. According to Yu et al. (2024), the dataset contains 1% P-phase and 4% S-phase outliers among the total 19,994 phase picks. Using a 0.2s threshold, ADLoc detected 184 (0.9%) P-phase and 539 (2.7%) S-phase outliers, matching the known outlier proportions. Examples of detected outliers are shown in Figure 4.

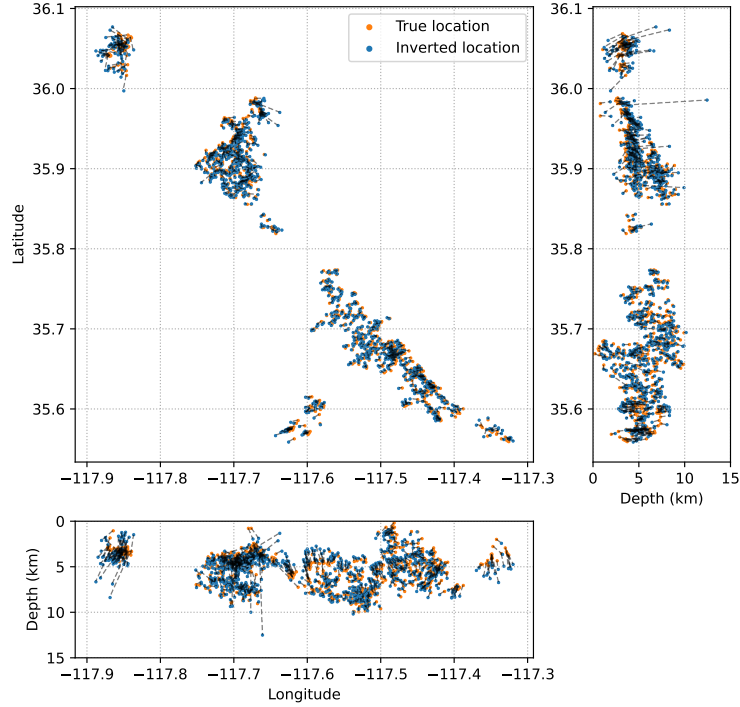


Figure 2: Comparison of estimated and true earthquake locations in the synthetic dataset.

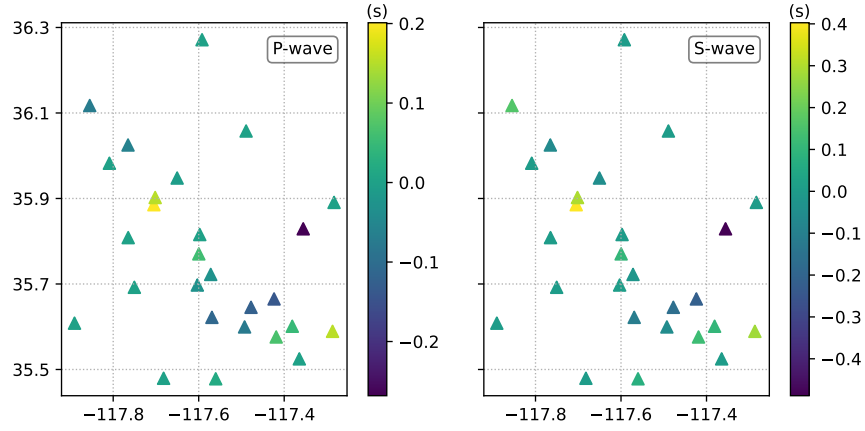


Figure 3: Estimated static station terms for P-wave and S wave.

Table 1: Quantitative comparison of location accuracy between different methods on the synthetic dataset. Lower values indicate better performance.

Method	Mean Accuracy Error (km)		Chamfer Distance
	Horizontal	Depth	
HypoInverse	0.824	1.118	1.617
VELEST	0.696	0.559	1.170
NonLinLoc	0.953	0.969	1.626
ADLoc	1.132	1.257	1.802
ADLoc+SST	0.680	0.539	1.080
ADLoc+SST+RANSAC (1.0s)	0.630	0.498	1.035
ADLoc+SST+RANSAC (0.2s)	0.456	0.450	0.915

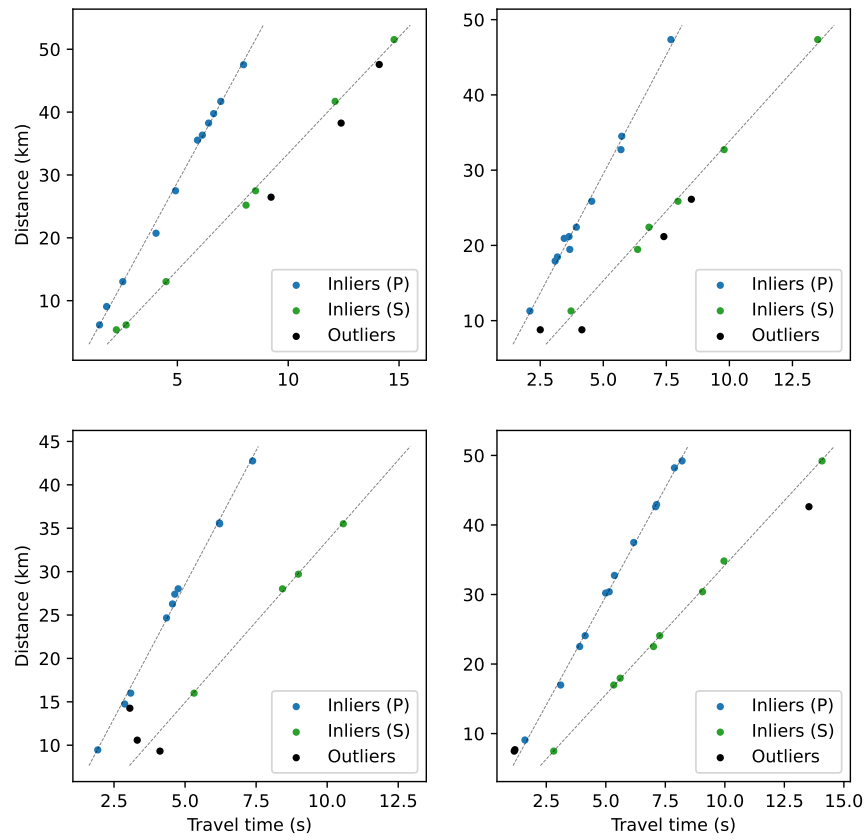


Figure 4: Examples of identified outlier picks.

Table 2: Hyperparameters for defining inlier picks and valid iterations in the RANSAC-based location method.

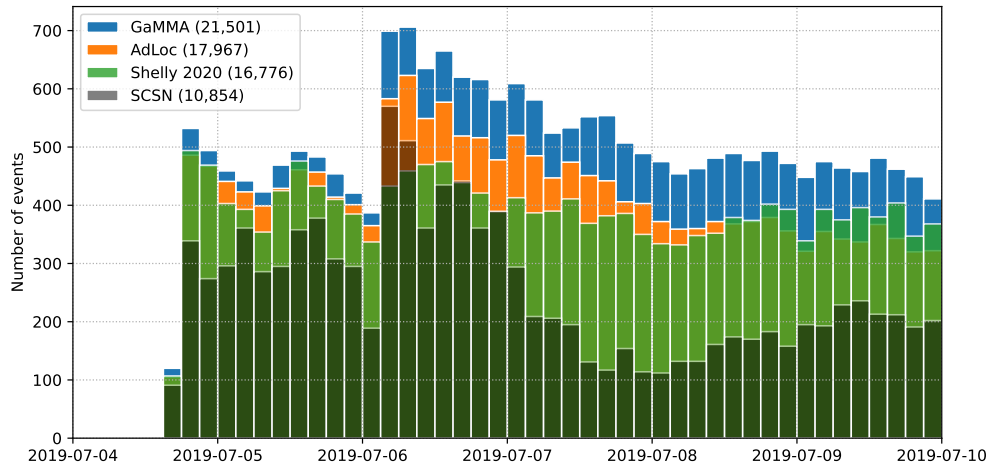
Hyperparameter	Value
Min picks	5
Min P-picks	1
Min S-picks	1
Max time residual (second)	1
Max amplitude residual (\log_{10} cm/s)	1
Min R^2 -score	0.6

3.2 Applications to real data

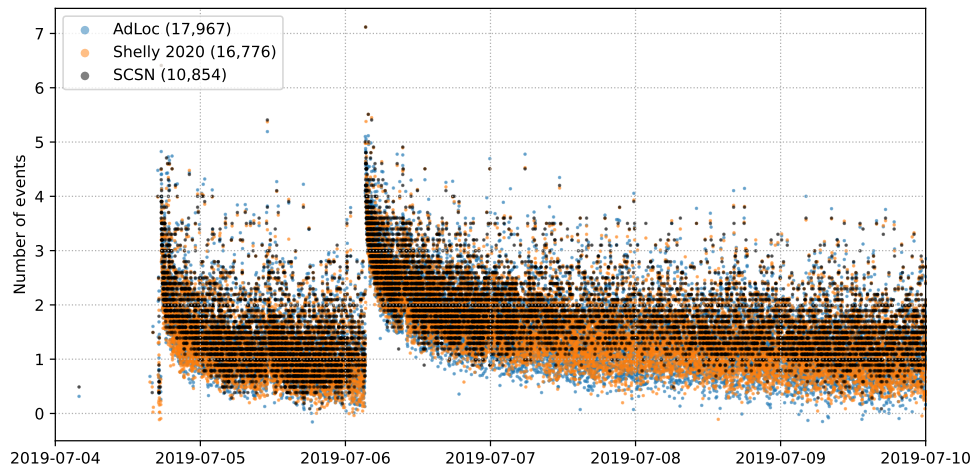
We further evaluated the RANSAC-based earthquake location method on the 2016 Ridgecrest earthquake sequence. This earthquake sequence is commonly used for evaluating earthquake catalogs due to its extensive aftershock activity and multiple comparison catalogs (Ross et al., 2019; Shelly, 2020a; White et al., 2021; M. Liu et al., 2020; Y. Zhou et al., 2023; Trugman, 2020). To facilitate reproducibility, we used the phase picks from W. Zhu et al. (2022), generated using a deep-learning-based phase picker, PhaseNet, and a Gaussian mixture model associator, GaMMA. We analyzed data from 07/04/2019–07/10/2019 within the same spatial extent as Shelly (2020b)’s catalog (-117.8°W to -117.3°W , 35.5°N to 36°N). The dataset includes 21,501 associated pick groups, comprising 452,702 P-phase and 463,217 S-phase picks. Unlike the synthetic dataset, this real dataset contains phase scores predicted by PhaseNet and measured PGV phase amplitudes, providing additional constraints for outlier detection and enhancing RANSAC robustness. Phase amplitude information improves outlier identification, particularly for false picks that align with travel-time moveouts but exhibit anomalous amplitudes. Phase scores are incorporated as weights in earthquake location (Equation (4)), station term estimation (Equation (6)), and the minimum pick counts in Table 2. Pick counts were determined by summing phase scores rather than raw counts, reducing the influence of low-quality picks. We applied a simplified ground motion prediction equation for PGV: $\log PGV = -2.175 - 1.68 \log R + 0.93M$ to fit the phase amplitude measurements, where R is hypocentral distance and M is magnitude (Picozzi et al., 2018). Other hyperparameters for defining inliers and outliers are listed in Table 2. Ten iterations were applied to estimate static station terms for both phase arrival-times and amplitudes. The estimated station correction terms and picks residuals of time and amplitude (Figures 8 and 9) show spatial correlation among the three station terms, and demonstrate zero mean, symmetric distributions of pick residuals. After RANSAC-based processing, 17,967 events were successfully located using 405,060 P-picks and 414,449 S-picks. We compared the catalog with the SCSN catalog and Shelly (2020b)’s catalog, which represent state-of-art in earthquake detection and location. Most events in the SCSN catalog have been manually reviewed, ensuring the catalog’s high quality during the aftershock period; and Shelly (2020b)’s catalog enhanced magnitude completeness and location accuracy through template matching and double-difference relocation. Although direct catalog comparisons remain challenging due to the absence of ground truth, Figures 5, 6 and 7 demonstrate consistency in spatial, temporal, and magnitude distributions, validating the effectiveness of ADLoc for complex earthquake sequence data. The ADLoc locations can be further refined through double-difference earthquake relocation using HypoDD (Waldhauser & Ellsworth, 2000) and Growclust (Trugman & Shearer, 2017) in future applications.

4 Discussion

RANSAC is a robust machine learning method designed to handle datasets containing many outliers by leveraging the assumption that a subset of samples can effectively constrain parameters. This assumption aligns well with earthquake location problems, which involve only four degrees of freedom (x, y, z, t) and require a minimum of four measurements. Through tests on synthetic and real data, we demonstrated the effectiveness of RANSAC-based earthquake location in environments with significant outliers in phase picks. RANSAC’s iterative random sampling and inlier detection enable effectively isolate false picks, reducing their impact on location estimates. This robustness is particularly valuable in low-magnitude earthquake scenarios where data quality and signal-to-noise ratios are poor, leading to more frequent false or inaccurate



(a)



(b)

Figure 5: Temporal distribution of detected earthquake events during the Ridgecrest sequence: (a) temporal distribution of earthquake frequency; (b) magnitude-time distribution of detected events.

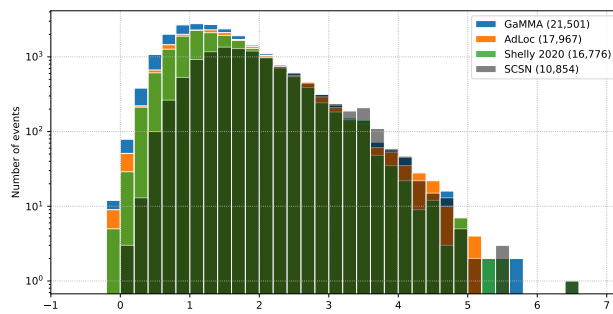


Figure 6: Magnitude distribution of detected events during the Ridgecrest sequence.

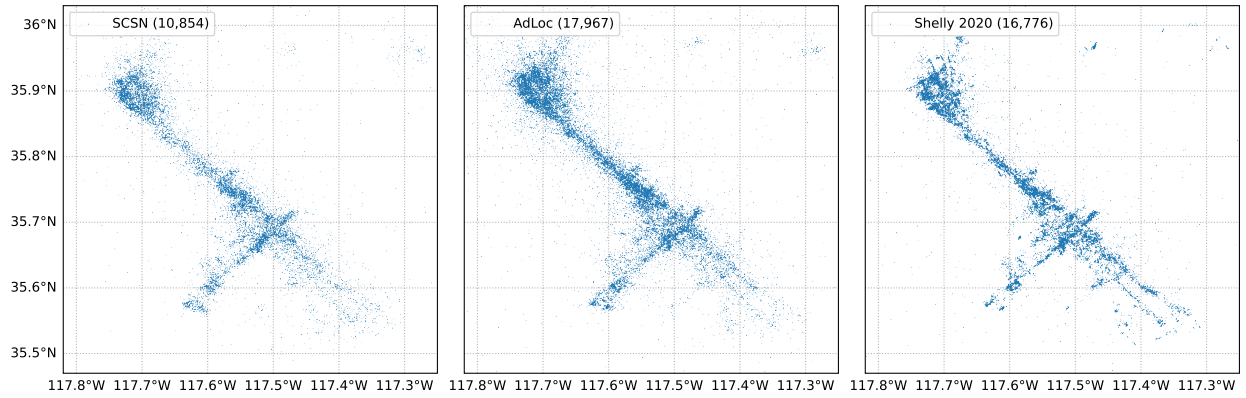


Figure 7: Spatial distribution of located events during the Ridgecrest sequence..

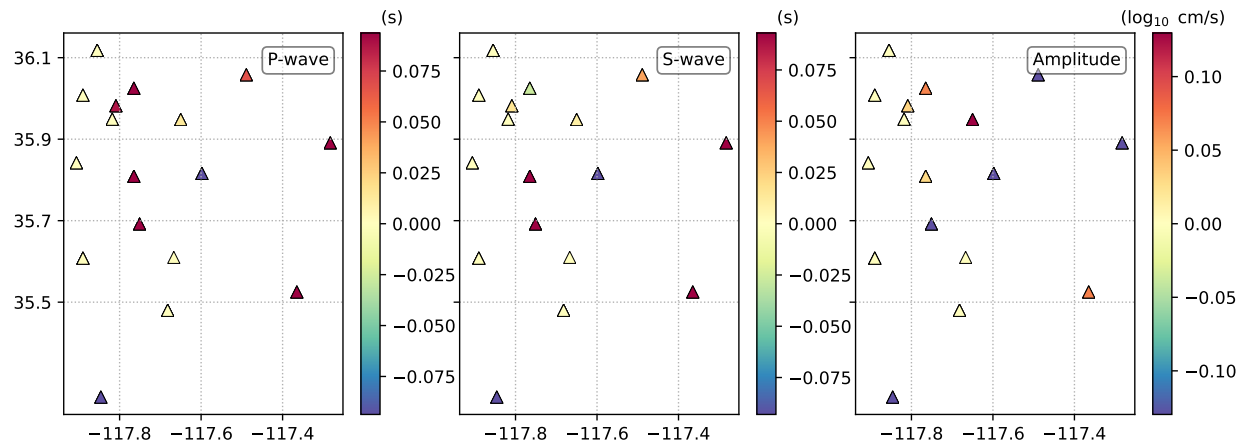


Figure 8: Estimated station correction terms for the Ridgecrest sequence showing (a) P-phase arrival-time corrections, (b) S-phase arrival-time corrections, and (c) amplitude corrections at each station.

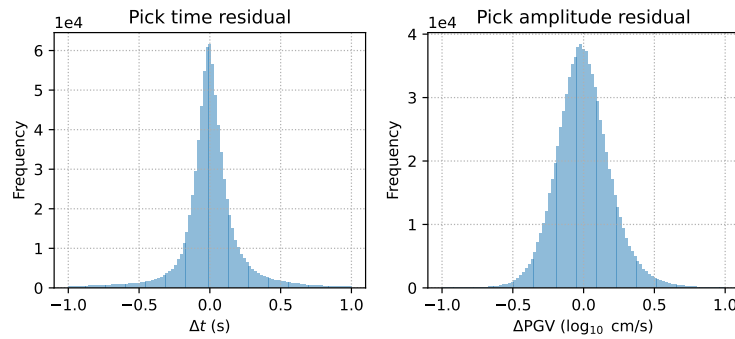


Figure 9: Distribution of pick residuals for (a) P-phase arrival times, (b) S-phase arrival times, and (c) phase amplitudes.

picks.

Despite its advantages, the RANSAC-based method has several limitations. The first is increased computational cost due to the random sampling process. The number of RANSAC iterations, N , is determined to ensure a high probability (P) of selecting at least one all-inlier subset:

$$N \geq \frac{\log(1 - P)}{\log(1 - R^s)} \quad (9)$$

where P is the probability of identifying an all-inlier subset, R is the fraction of inliers in the dataset, and s is the subset size. Common values include $P = 0.99$, with R estimated from the dataset, and s set to the minimum number of picks required for valid earthquake location (Table 2). If no outliers exist, only one iteration is required, and the computational cost reverts to that of traditional earthquake location methods. However, datasets with more outliers necessitate additional iterations and increased computational costs to achieve reliable results. The inlier fraction is dynamically estimated during iterations, and as location accuracy improves, the inlier fraction increases, reducing the maximum required iterations. This iterative refinement allows the algorithm to quickly converge to an all-inlier subset. In practice, a cap on the maximum number of iterations is imposed to control computational expense.

The second limitation is the dependence on hyperparameters for defining outliers. The hyperparameters listed in Table 2 provide flexibility to optimize location quality but also introduce sensitivity to parameter settings. Synthetic tests (Table 1) indicate that tighter thresholds on maximum time residual enable more effective outlier detection, thereby enhancing location accuracy. However, real-world applications require careful tuning of these thresholds to balance the trade-off between the number of successfully located earthquakes and the accuracy of their locations. When applied to the Ridgecrest sequence, these limitations have minimal impact. The method processes 24,479 events with 1,005,388 picks in approximately 1.5 minutes using 32 cores, and the default hyperparameters yield consistent and reliable location results.

Last, while the RANSAC iterations improve robustness to outliers, they do not guarantee an optimal solution for earthquake location. The core location step, which minimizes travel-time residuals (Step 3), remains the same as in traditional earthquake location methods. Therefore, the RANSAC-based framework still inherits limitations of traditional methods, such as potential convergence to local minima, trade-offs between event depth and origin time, and biases from inaccurate velocity models. On the other hand, the RANSAC framework’s adaptability allows integration of improvements in both RANSAC and earthquake location algorithms. Our implementation demonstrates this through the successful integration of static station corrections and phase amplitude-based outlier detection. Moreover, alternative RANSAC extensions, such as MLESAC (Maximum Likelihood Estimation Sample Consensus) (Torr & Zisserman, 2000), could enhance the inlier detection process by incorporating probabilistic approaches instead of hard threshold. Integrating uncertainty estimation frameworks into the RANSAC process could enhance robust earthquake localization in future research.

5 Conclusions

Advances in seismic monitoring and machine learning have significantly improved the detection of small-magnitude earthquakes, while introducing new challenges in robust earthquake location due to increased false or inaccurate phase picks. We have introduced a robust earthquake location framework that integrates the Random Sample Consensus (RANSAC) algorithm with traditional location techniques. The framework enhances robustness against outliers through iterative sampling and outlier detection and is adaptable to further improvements, such as static station corrections and amplitude-based outlier detection. Through validation with synthetic experiments and application to the Ridgecrest earthquake sequence, the framework has demonstrated consistent performance and enhanced accuracy in outlier-prone scenarios. The RANSAC-based framework offers a robust and flexible solution to balance the trade-off between expanding earthquake catalogs and maintaining data quality. This approach contributes to the development of higher-quality earthquake catalogs, enabling precise earthquake characterization and supporting a wide range of geophysical studies.

Acknowledgments

We thank Yifan Yu for sharing the benchmark earthquake location tests (Yu et al., 2024) and helping with the calculation of location resolution metrics. The ADLoc source code is available on GitHub at <https://github.com/AI4EPS/ADLoc>

References

- Aki, K., & Lee, W. (1976). Determination of three-dimensional velocity anomalies under a seismic array using first p arrival times from local earthquakes: 1. a homogeneous initial model. *Journal of Geophysical research*, *81*(23), 4381–4399.
- Allen, R. M., Gasparini, P., Kamigaichi, O., & Bose, M. (2009). The status of earthquake early warning around the world: An introductory overview. *Seismological Research Letters*, *80*(5), 682–693.
- Anderson, K. R. (1982). Robust earthquake location using m-estimates. *Physics of the Earth and Planetary Interiors*, *30*(2-3), 119–130.
- Baydin, A. G., Pearlmutter, B. A., Radul, A. A., & Siskind, J. M. (2018). Automatic differentiation in machine learning: a survey. *Journal of machine learning research*, *18*(153), 1–43.
- Byrd, R. H., Lu, P., Nocedal, J., & Zhu, C. (1995). A limited memory algorithm for bound constrained optimization. *SIAM Journal on scientific computing*, *16*(5), 1190–1208.
- Červený, V., & Pšenčík, I. (2020). Seismic ray theory. *Encyclopedia of solid earth geophysics*, 1–17.
- Douglas, A. (1967, July). Joint epicentre determination. *Nature*, *215*(5096), 47–48.
- Ellsworth, W. L. (1975). Bear valley, california, earthquake sequence of February-march 1972. *Bulletin of the Seismological Society of America*, *65*(2), 483–506.
- Ellsworth, W. L. (2013). Injection-induced earthquakes. *science*, *341*(6142), 1225942.
- Fadakar Alghalandis, Y., Dowd, P. A., & Xu, C. (2013). The RANSAC method for generating fracture networks from micro-seismic event data. *Mathematical Geosciences*, *45*, 207–224.
- Faulkner, D., Jackson, C., Lunn, R., Schlische, R., Shipton, Z., Wibberley, C., & Withjack, M. (2010). A review of recent developments concerning the structure, mechanics and fluid flow properties of fault zones. *Journal of Structural Geology*, *32*(11), 1557–1575.
- Fischler, M. A., & Bolles, R. C. (1981). Random sample consensus: A paradigm for model fitting with applications to image analysis and automated cartography. *Communications of the ACM*, *24*(6), 381–395.
- Font, Y., Kao, H., Lallemand, S., Liu, C.-S., & Chiao, L.-Y. (2004). Hypocentre determination offshore of eastern taiwan using the maximum intersection method. *Geophysical Journal International*, *158*(2), 655–675.
- Frohlich, C. (1979). An efficient method for joint hypocenter determination for large groups of earthquakes. *Computers & Geosciences*, *5*(3-4), 387–389.
- Geiger, L. (1912). Probability method for the determination of earthquake epicentres from the arrival time only. *Bull. St. Louis Univ.*, *8*, 60.
- Hartley, R., & Zisserman, A. (2003). *Multiple view geometry in computer vision*. Cambridge university press.
- Hauksson, E., Yang, W., & Shearer, P. M. (2012). Waveform relocated earthquake catalog for southern california (1981 to june 2011). *Bulletin of the Seismological Society of America*, *102*(5), 2239–2244.
- Hirata, N., & Matsu’ura, M. (1987, August). Maximum-likelihood estimation of hypocenter with origin time eliminated using nonlinear inversion technique. *Physics of the Earth and Planetary Interiors*, *47*, 50–61.
- Huber, P. J. (1964). Robust estimation of a location parameter. *The Annals of Mathematical Statistics*, *35*(1), 73–101.

- Hutton, K., Woessner, J., & Hauksson, E. (2010, April). Earthquake Monitoring in Southern California for Seventy-Seven Years (1932-2008). *Bulletin of the Seismological Society of America*, 100(2), 423–446.
- Kanamori, H. (2005). Real-time seismology and earthquake damage mitigation. *Annu. Rev. Earth Planet. Sci.*, 33(1), 195–214.
- Kanamori, H., & Brodsky, E. E. (2004). The physics of earthquakes. *Reports on progress in physics*, 67(8), 1429.
- Kissling, E., Ellsworth, W. L., Eberhart-Phillips, D., & Kradolfer, U. (1994). Initial reference models in local earthquake tomography. *Journal of Geophysical Research: Solid Earth*, 99(B10), 19635–19646.
- Klein, F. W. (2002). *User’s guide to HYPOINVERSE-2000, a fortran program to solve for earthquake locations and magnitudes* (Tech. Rep. No. 2002-171). U.S. Geological Survey.
- Lahr, J. C. (1979). *HYPOELLIPSE/MULTICS: A computer program for determining local earthquake hypocentral parameters, magnitude, and first motion pattern* (Tech. Rep.). US Geological Survey.
- Lee, W. H., & Lahr, J. C. (1975). *HYPO71 (revised; a computer program for determining hypocenter, magnitude, and first motion pattern of local earthquakes* (Tech. Rep.). US Dept. of the Interior, Geological Survey, National Center for Earthquake
- Lin, G. (2018, September). The Source-Specific Station Term and Waveform Cross-Correlation Earthquake Location Package and Its Applications to California and New Zealand. *Seismological Research Letters*, 89(5), 1877–1885.
- Lin, G., & Shearer, P. (2006, July). The COMLOC Earthquake Location Package. *Seismological Research Letters*, 77(4), 440–444.
- Liu, M., Zhang, M., Zhu, W., Ellsworth, W. L., & Li, H. (2020). Rapid characterization of the July 2019 ridgecrest, California, earthquake sequence from raw seismic data using machine-learning phase picker. *Geophysical Research Letters*, 47(4), e2019GL086189.
- Liu, X., Jin, Y., Lin, B., Xiang, J., & Zhong, H. (2018). An enhanced RANSAC method for complex hydraulic network characterization based on microseismic data. In *ARMA international discrete fracture network engineering conference* (p. D023S014R010). ARMA.
- Lomax, A. (2005). A reanalysis of the hypocentral location and related observations for the great 1906 California earthquake. *Bulletin of the Seismological Society of America*, 95(3), 861–877.
- Lomax, A., Michelini, A., & Curtis, A. (2009). Earthquake location, direct, global-search methods. , 25.
- Lomax, A., & Savvaidis, A. (2022). High-precision earthquake location using source-specific station terms and inter-event waveform similarity. *Journal of Geophysical Research: Solid Earth*, 127(1), e2021JB023190.
- Lomax, A., Virieux, J., Volant, P., & Berge-Thierry, C. (2000). Probabilistic earthquake location in 3D and layered models. In C. H. Thurber & N. Rabinowitz (Eds.), *Advances in Seismic Event Location* (pp. 101–134). Dordrecht: Springer Netherlands.
- Mousavi, S. M., Ellsworth, W. L., Zhu, W., Chuang, L. Y., & Beroza, G. C. (2020). Earthquake transformer—an attentive deep-learning model for simultaneous earthquake detection and phase picking. *Nature communications*, 11(1), 3952.
- Myers, S. C., Johannesson, G., & Hanley, W. (2007). A bayesian hierarchical method for multiple-event seismic location. *Geophysical Journal International*, 171(3), 1049–1063.
- Nocedal, J., & Wright, S. J. (1999). *Numerical optimization*. Springer.
- Park, Y., Beroza, G. C., & Ellsworth, W. L. (2022). Basement fault activation before larger earthquakes in Oklahoma and Kansas. *The Seismic Record*, 2(3), 197–206.

- Paszke, A., Gross, S., Chintala, S., Chanan, G., Yang, E., DeVito, Z., ... Lerer, A. (2017). Automatic differentiation in pytorch.
- Picozzi, M., Bindi, D., Spallarossa, D., Di Giacomo, D., & Zollo, A. (2018). A rapid response magnitude scale for timely assessment of the high frequency seismic radiation. *Scientific reports*, 8(1), 8562.
- Podvin, P., & Lecomte, I. (1991). Finite difference computation of traveltimes in very contrasted velocity models: a massively parallel approach and its associated tools. *Geophysical Journal International*, 105(1), 271–284.
- Pollitz, F. F., Wicks, C., Schoenball, M., Ellsworth, W., & Murray, M. (2017). Geodetic slip model of the 3 september 2016 M w 5.8 pawnee, oklahoma, earthquake: Evidence for fault-zone collapse. *Seismological Research Letters*, 88(4), 983–993.
- Pujol, J. (1988). Comments on the joint determination of hypocenters and station corrections. *Bulletin of the Seismological Society of America*, 78(3), 1179–1189.
- Richards-Dinger, K., & Shearer, P. (2000). Earthquake locations in southern california obtained using source-specific station terms. *Journal of Geophysical Research: Solid Earth*, 105(B5), 10939–10960.
- Ross, Z. E., Cochran, E. S., Trugman, D. T., & Smith, J. D. (2020). 3d fault architecture controls the dynamism of earthquake swarms. *Science*, 368(6497), 1357–1361.
- Ross, Z. E., Idini, B., Jia, Z., Stephenson, O. L., Zhong, M., Wang, X., ... others (2019). Hierarchical interlocked orthogonal faulting in the 2019 ridgecrest earthquake sequence. *Science*, 366(6463), 346–351.
- Ross, Z. E., Meier, M.-A., & Hauksson, E. (2018). P wave arrival picking and first-motion polarity determination with deep learning. *Journal of Geophysical Research: Solid Earth*, 123(6), 5120–5129.
- Shearer, P., Hauksson, E., & Lin, G. (2005). Southern california hypocenter relocation with waveform cross-correlation, part 2: Results using source-specific station terms and cluster analysis. *Bulletin of the Seismological Society of America*, 95(3), 904–915.
- Shearer, P. M. (1997). Improving local earthquake locations using the l1 norm and waveform cross correlation: Application to the whittier narrows, california, aftershock sequence. *Journal of Geophysical Research: Solid Earth*, 102(B4), 8269–8283.
- Shelly, D. R. (2020a). A high-resolution seismic catalog for the initial 2019 ridgecrest earthquake sequence: Foreshocks, aftershocks, and faulting complexity. *Seismological Research Letters*, 91(4), 1971–1978.
- Shelly, D. R. (2020b, January). A High-Resolution Seismic Catalog for the Initial 2019 Ridgecrest Earthquake Sequence: Foreshocks, Aftershocks, and Faulting Complexity. *Seismological Research Letters*, 91(4), 1971–1978.
- Shelly, D. R., Ellsworth, W. L., & Hill, D. P. (2016). Fluid-faulting evolution in high definition: Connecting fault structure and frequency-magnitude variations during the 2014 long valley caldera, california, earthquake swarm. *Journal of Geophysical Research: Solid Earth*, 121(3), 1776–1795.
- Skoumal, R. J., Kaven, J. O., & Walter, J. I. (2019). Characterizing seismogenic fault structures in oklahoma using a relocated template-matched catalog. *Seismological Research Letters*, 90(4), 1535–1543.
- Smith, J. D., Azizzadenesheli, K., & Ross, Z. E. (2020). Eikonet: Solving the eikonal equation with deep neural networks. *IEEE Transactions on Geoscience and Remote Sensing*, 59(12), 10685–10696.
- Smith, J. D., Ross, Z. E., Azizzadenesheli, K., & Muir, J. B. (2022, January). HypoSVI: Hypocentre inversion with Stein variational inference and physics informed neural networks. *Geophysical Journal International*, 228(1), 698–710.
- Sun, H., Ross, Z. E., Zhu, W., & Azizzadenesheli, K. (2023). Phase neural operator for multi-station picking of seismic arrivals. *Geophysical Research Letters*, 50(24), e2023GL106434.

- Szeliski, R. (2022). *Computer vision: algorithms and applications*. Springer Nature.
- Thurber, C. H. (1983). Earthquake locations and three-dimensional crustal structure in the coyote lake area, central california. *Journal of Geophysical Research: Solid Earth*, 88(B10), 8226–8236.
- Thurber, C. H. (1985, June). Nonlinear earthquake location: Theory and examples. *Bulletin of the Seismological Society of America*, 75(3), 779–790.
- Thurber, C. H. (1992, December). Hypocenter-velocity structure coupling in local earthquake tomography. *Physics of the Earth and Planetary Interiors*, 75(1), 55–62.
- Tong, P. (2021). Adjoint-state travelttime tomography: Eikonal equation-based methods and application to the anza area in southern california. *Journal of Geophysical Research: Solid Earth*, 126(5), e2021JB021818.
- Torr, P. H., & Zisserman, A. (2000). Mlesac: A new robust estimator with application to estimating image geometry. *Computer vision and image understanding*, 78(1), 138–156.
- Trugman, D. T. (2020). Stress-drop and source scaling of the 2019 ridgecrest, california, earthquake sequence. *Bulletin of the Seismological Society of America*, 110(4), 1859–1871.
- Trugman, D. T. (2024). A high-precision earthquake catalog for nevada. *Seismological Research Letters*, 95(6), 3737–3745.
- Trugman, D. T., McBrearty, I. W., Bolton, D. C., Guyer, R. A., Marone, C., & Johnson, P. A. (2020). The spatiotemporal evolution of granular microslip precursors to laboratory earthquakes. *Geophysical Research Letters*, 47(16), e2020GL088404.
- Trugman, D. T., & Shearer, P. M. (2017, February). GrowClust: A Hierarchical Clustering Algorithm for Relative Earthquake Relocation, with Application to the Spanish Springs and Sheldon, Nevada, Earthquake Sequences. *Seismological Research Letters*, 88(2A), 379–391.
- Um, J., & Thurber, C. (1987). A fast algorithm for two-point seismic ray tracing. *Bulletin of the Seismological Society of America*, 77(3), 972–986.
- Van Trier, J., & Symes, W. W. (1991). Upwind finite-difference calculation of traveltimes. *Geophysics*, 56(6), 812–821.
- Vidale, J. (1988). Finite-difference calculation of travel times. *Bulletin of the seismological society of America*, 78(6), 2062–2076.
- Waldhauser, F. (2001). *Hypodd-a program to compute double-difference hypocenter locations* (Tech. Rep.).
- Waldhauser, F., & Ellsworth, W. L. (2000, December). A Double-Difference Earthquake Location Algorithm: Method and Application to the Northern Hayward Fault, California. *Bulletin of the Seismological Society of America*, 90(6), 1353–1368.
- Waldhauser, F., & Ellsworth, W. L. (2002). Fault structure and mechanics of the hayward fault, california, from double-difference earthquake locations. *Journal of Geophysical Research: Solid Earth*, 107(B3), ESE–3.
- Waldhauser, F., & Schaff, D. P. (2008). Large-scale relocation of two decades of northern california seismicity using cross-correlation and double-difference methods. *Journal of Geophysical Research: Solid Earth*, 113(B8).
- White, M. C., Fang, H., Catchings, R. D., Goldman, M. R., Steidl, J. H., & Ben-Zion, Y. (2021). Detailed travelttime tomography and seismic catalogue around the 2019 m w7. 1 ridgecrest, california, earthquake using dense rapid-response seismic data. *Geophysical Journal International*, 227(1), 204–227.

- White, M. C., Fang, H., Nakata, N., & Ben-Zion, Y. (2020). Pykonal: a python package for solving the eikonal equation in spherical and cartesian coordinates using the fast marching method. *Seismological Research Letters*, 91(4), 2378–2389.
- Wilding, J. D., Zhu, W., Ross, Z. E., & Jackson, J. M. (2023). The magmatic web beneath hawaii ‘i. *Science*, 379(6631), 462–468.
- Woollam, J., Rietbrock, A., Leitloff, J., & Hinz, S. (2020, July). HEX: Hyperbolic Event eXtractor, a Seismic Phase Associator for Highly Active Seismic Regions. *Seismological Research Letters*, 91(5), 2769–2778.
- Yu, Y., Ellsworth, W. L., & Beroza, G. C. (2024). Accuracy and precision of earthquake location programs: Insights from a synthetic controlled experiment. *Seismological Research Letters (submitted)*, year.
- Zhao, D., Hasegawa, A., & Horiuchi, S. (1992). Tomographic imaging of p and s wave velocity structure beneath northeastern japan. *Journal of Geophysical Research: Solid Earth*, 97(B13), 19909–19928.
- Zhao, H. (2005). A fast sweeping method for eikonal equations. *Mathematics of Computation*, 74(250), 603–627.
- Zhou, H.-w. (1994). Rapid three-dimensional hypocentral determination using a master station method. *Journal of Geophysical Research: Solid Earth*, 99(B8), 15439–15455.
- Zhou, Y., Ghosh, A., Fang, L., Yue, H., & Zhou, S. (2023). Construction of long-term seismic catalog with deep learning and characterization of preseismic fault behavior in the ridgecrest-coso region (2008-2019). *Authorea Preprints*.
- Zhu, L., Chuang, L., McClellan, J. H., Liu, E., & Peng, Z. (2021, July). A multi-channel approach for automatic microseismic event association using RANSAC-based arrival time event clustering (RATEC). *Earthquake Research Advances*, 1(3), 100008.
- Zhu, L., Liu, E., & McClellan, J. (2016). An automatic arrival time picking method based on RANSAC curve fitting. In *78th EAGE conference and exhibition 2016* (Vol. 2016, pp. 1–5). European Association of Geoscientists & Engineers.
- Zhu, L., Liu, E., McClellan, J., Zhao, Y., Li, W., Li, Z., & Peng, Z. (2017). Estimation of passive microseismic event location using random sampling-based curve fitting. In *SEG international exposition and annual meeting* (pp. SEG–2017). SEG.
- Zhu, W., & Beroza, G. C. (2019). Phasenet: a deep-neural-network-based seismic arrival-time picking method. *Geophysical Journal International*, 216(1), 261–273.
- Zhu, W., McBrearty, I. W., Mousavi, S. M., Ellsworth, W. L., & Beroza, G. C. (2022). Earthquake phase association using a bayesian gaussian mixture model. *Journal of Geophysical Research: Solid Earth*, 127(5), e2021JB023249.
- Zhu, W., Xu, K., Darve, E., & Beroza, G. C. (2021). A general approach to seismic inversion with automatic differentiation. *Computers & Geosciences*, 151, 104751.